Peer-reviewed version available at Processes 2018, 6, 23; doi:10.3390/pr6030023

Article

Fuel Gas Network Synthesis Using Block Superstructure

Jianping Li, Salih Emre Demirel and M. M. Faruque Hasan*

Artie McFerrin Department of Chemical Engineering, Texas A&M University, College Station, TX 77843-3122, USA.; ljptamu@tamu.edu; emredemirel@tamu.edu

* Correspondence: hasan@tamu.edu; Tel.: +1-979-862-1449

Abstract: Fuel gas network (FGN) synthesis is a systematic method for reducing fresh fuel consumption in a chemical plant. In this work, we address the synthesis of fuel gas network using block superstructure originally proposed for process design and intensification (Demirel et.al. [1]). Instead of a classical source-pool-sink superstructure, we consider a superstructure with multiple feed and product streams. These blocks interact with each other through direct flows that connect a block with its adjacent blocks and through jump flows that connect a block with all blocks. The blocks with feed streams are viewed as fuel sources and the blocks with product streams are regarded as fuel sinks. Addition blocks can be added as pools when there exists intermediate operations among source blocks and sink blocks. These blocks can be arranged in a $I \times J$ two-dimensional grid with $I = 1$ for problems without pools, or $I = 2$ for problems with pools. J is determined by the maximum number of pools/sinks. With this representation, we formulate fuel gas network synthesis problem as a mixed-integer nonlinear (MINLP) problem to optimally design a fuel gas network with minimal total annul cost. We present a real-life case study from LNG plant to demonstrate the capability of the proposed approach.

Keywords: process integration, fuel gas network synthesis, block superstructure, optimization, MINLP

1. Introduction

Over 40% of the operating cost of a petrochemical plant is attributed to energy consumption [2]. Energy is needed for raw material preprocessing (preheating, purification), separation of products from intermediates or impurities (product refining), and material transportation. There are multiple energy sources that can be exploited in a refinery, such as liquefied petroleum gases, fuel gas, off-gas, etc. [3,4]. These energy sources either come from external process raw materials/purchased fuels or from internal process /products/byproducts. Depending on where these fuel sources originate from, they can be divided as fuel from feed (natural gas) or fuel from product (products, byproducts) [5]. In 2016, external fuels supplied to refinery industry in the United States mainly consist of natural gas (31%), electricity (5%), purchased steam and coal (1%) [6]. About 63% of the energy consumed by the refinery industry comes from byproducts of the refining process for heat and power. These energy sources sometimes may be convertible to each other. For example, fuel gas, produced internally from the distillation columns, crackers and reformers [7], can be converted to other forms of energy such as steam, electricity and heat. Fuel gas accounts for 46% among all energy sources of refinery industry in the United States in 2016 [6]. As a result, it contributes most of primary energy sources to refinery energy needs [8–10]. Fuel gas is often composed of hydrocarbons (methane, ethane, propane and butane), hydrogen, and carbon monoxide, which have large heating values [11]. In most cases, these fuels are flared to the atmosphere, which has detrimental effect on the environment [12,13].

Due to the importance of fuel gas and the environment concern of fuel gas emission, many efforts have been made on improving the equipment efficiency [14] or exploiting new energy sources to

Preprints (www.preprints.org) | NOT PEER-REVIEWED | Posted: 5 February 2018 doi:10.20944/preprints201802.0025.v1

Peer-reviewed version available at Processes 2018, 6, 23; doi:10.3390/pr6030023

decrease fuel gas generation and pollution emission [15]. Although these works give insights and directions on improving design of equipment and operating conditions, a general and systematic strategy for elucidating the effective utilization of fuel gas is crucial. For example, in a typical fuel gas system, multiple fuel gas sources with different qualities are available for various equipment (sinks). As a result, effective management of fuel gas flow among fuel gas sources and fuel gas sinks can provide economic benefits for process design by fully utilizing the heating value embedded in the fuel gas. A system level, integration, is required to account for various interactions within the fuel gas system [16,17].

Optimization-based methods enable to address fuel gas network (FGN) synthesis problems, which aims at redistributing the fuel gas at the system level [2,5,18]. To this end, Hasan et al. formalized the FGN synthesis problem as a nonlinear programming problem (NLP) considering the integration of fuel gases appropriately though auxiliary equipment (valves, pipelines, compressors, heaters/coolers, etc.) to achieve best utilization of them [5]. They posed the FGN problem as a special class of pooling problem which leads a superstructure as shown in Figure 1 involving many practical features such as nonisobaric and nonisothermal operation, nonisothermal mixing, nonlinear fuel-quality specifications, and emission standards. Jagannath et al. [18] extended this work to include the multi-period FGN operation. This FGN design makes dynamic plant operation more robust and helps to reduce capital costs. Nassim et al. [2,19] modified the FGN model introduced by Hasan et al. [5] to include more constraints on addressing environmental issues and developed a novel methodology for grass-root and retrofit design of FGNs.

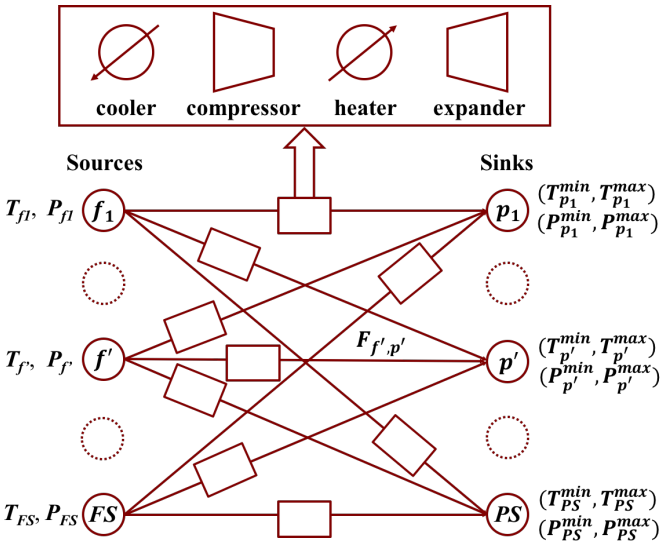

Figure 1. Superstructure for a fuel gas network proposed by Hasan et.al [5].

The first step for many optimization-based methods is the construction of a superstructure. Hence the appropriate selection of superstructure representation method is critical. There are many representations such as state-task-network [20,21], state-equipment-network [21], P-graph [22,23], state-space [24,25] , and unit-port-conditioning-stream (UPCS) approach [26,27]. We recently proposed a new superstructure representation method using building blocks for systematic process intensification [1,28,29]. The block superstructure has been constructed based on the dissection of various unit operations into fundamental building blocks. Later on, the proposed block-based approach is applied to address process synthesis problems [30].

In this work, we address the optimal synthesis of fuel gas networks using a block superstructure, originally proposed in our previous work for process synthesis and intensification [1,28,30]. Since fuel gas network by its definition is a special class of pooling problem, our block representation method can be extended to general pooling problems as well. In this representation, each block

allows multiple fuel gas inlet flows and single product outlet flow (unique composition for different product streams). The blocks with external feeds and external products serve as sources and sinks for fuel gas respectively. The material and energy flow among different blocks are achieved via jump flow streams connecting all blocks with each other and direct connecting streams connecting only adjacent blocks. The involvement of jump flows is a novelty of this work that avoids the utilization of unnecessary intermediate blocks for inter-block connections. Each stream connecting two adjacent blocks are placed with compressors/expanders to adjust the pressure for achieving the sink requirements. Options for supplying extra hot/cold utility are provided to each block for allowing nonisothermal operation. When there is no direct connecting stream, the block boundary between adjacent blocks is regarded as completely restricted boundary. These blocks are collected in a two-dimensional grid to form a superstructure of blocks. We formulate the fuel gas synthesis problem as a mixed-integer nonlinear optimization (MINLP) problem. The model constraints involve mass and energy balance, flow directions, work calculation and logic constraints. The nonlinear terms of the proposed model arise from splitting, energy balances and work-related calculations.

The remaining of the article is structured as follows. First, we elaborate the representation of fuel gas network using block-based approach. Next, we present the MINLP formulation for fuel gas network synthesis problem. Finally, we demonstrate the applicability of our approach with one case study from LNG plant.

2. Block-based Representation of Fuel Gas Network

In this section, we describe how the classic fuel gas network superstructure such as the one proposed by Hasan et al. [5] can be represented using block-based approach [1,30] as a generic tool for designing fuel gas utilization system. First, we illustrate the classical FGN superstructure and analyze the operation involved in synthesizing a FGN. Next, we construct a block superstructure that also can include the same features. We provide block superstructures for fuel gas network with or without intermediate pools which bring additional mixing operations for more economic benefits.

In a classical FGN superstructure (Hasan et.al [5]), shown in Figure 1, there are FS number of fuel gas sources and PS number of fuel gas sinks. The source stream f has the temperature as T_f and the pressure as P_f. The sink stream p is obtained with temperature range as $\left[T_p^{min}, T_p^{max}\right]$ and pressure range as $\left[P_p^{min}, P_p^{max}\right]$. Each stream $F_{f,p}$ connecting a source f and a sink p passes through two utility exchangers (heater and/or cooler) and one mover (compressor or expander). The sources completely or partially come from different fuel gas sources and are mixed at different fuel gas sinks with different temperature, pressure and quality requirements. The operations in a FGN problem typically include mixing, cooling, heating, pressurizing and depressurizing.

Most FGN synthesis problems involve multiple sources and multiple sinks. In addition, there are similar equipment assignment that are assigned between sources and sinks. This allows us to develop a general block representation for FGN synthesis as shown in Figure 2. It involves I number of rows and J number of columns, where each row or column is a collection of blocks. Let $B_{i,j}$ represent the block at row i and column j. Each block allows multiple feed streams $M_{i,j,k,f}$ to enter block $B_{i,j}$. The available amount of feed f can be partially or completely fed into a block $B_{i,j}$ with $z_{i,j,f}^{feedfrac}$ fraction of available amount F_f^{feed}. Similarly, product stream p can be withdrawn from each block with the component flowrate of $H_{i,j,k,p}$.

Preprints (www.preprints.org) | NOT PEER-REVIEWED | Posted: 5 February 2018 doi:10.20944/preprints201802.0025.v1

Peer-reviewed version available at Processes 2018, 6, 23; doi:10.3390/pr6030023

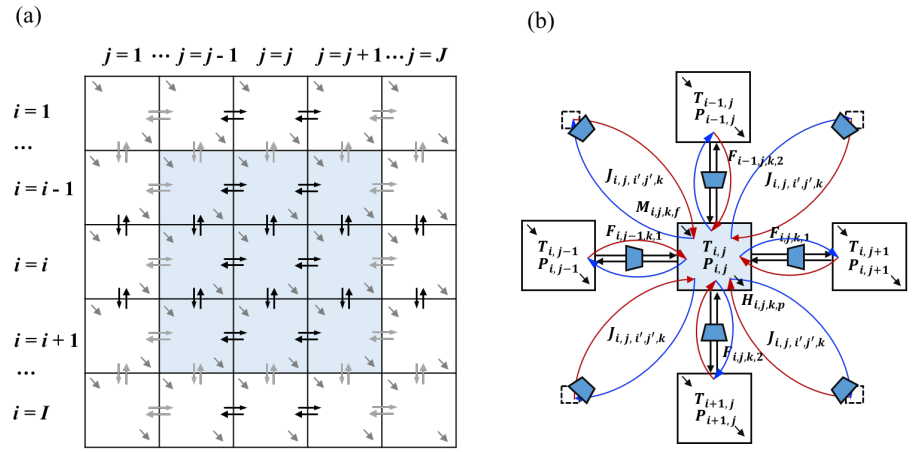

Figure 2. Construction of superstructure for fuel gas synthesis problems: **(a)** Block superstructure illustration. **(b)** Block interaction through via connecting streams (blue line: jump product from the block $B_{i,j}$; red line: jump feed into the block $B_{i,j}$; blocks at diagonal positions are ignored for simplicity).

As shown in Figure 2b, the mass and energy transfer within the block superstructure is achieved through the direct connecting streams between adjacent blocks and jump connecting streams among all blocks. Direct connecting streams are achieved via inter-block flow $F_{i,j,k,d}$, which is the flowrate of component k between block $B_{i,j}$ and $B_{i,j+1}$ when the flow alignment $d = 1$ (the connecting flow between adjacent blocks is in horizontal direction) or the flowrate of component k between block $B_{i,j}$ and $B_{i+1,j}$ when the flow alignment $d = 2$ (the connecting flow between adjacent blocks is in vertical direction) . These direct connecting streams can be either positive when the flow is from block $B_{i,j}$ to $B_{i,j+1}$ for $d = 1$ (from block $B_{i,j}$ to $B_{i+1,j}$ for $d = 2$) or negative when the flow is from block $B_{i,j+1}$ to $B_{i,j}$ for $d = 1$ (from block $B_{i+1,j}$ to $B_{i,j}$ for $d = 2$). Also, these direct connecting stream flow across the block boundary between adjacent blocks. When there is no direct connecting stream ($F_{i,j,k,d} = 0$), the block boundary between $B_{i,j}$ and $B_{i,j+1}$ (d=1) or between $B_{i,j}$ and $B_{i+1,j}$ (d=2) is identified as completely restricted boundary. The jump connecting streams are depicted by $J_{i,j,i',j',k}$, which is the flowrate of component k from block $B_{i,j}$ to $B_{i',j'}$, where i' and j' designate the row number and column number of a different block. Because of this unidirectional feature, $J_{i,j,i',j',k}$ is regarded as an jump product withdrawn from $B_{i,j}$. Similarly, $J_{i,j,i',j',k}$ is regarded as an jump feed supplied to $B_{i',j'}$.

With these direct and jump connecting streams, blocks with multiple inlets and multiple outlets can serve as stream mixers and splitters, respectively. Source block is identified when multiple external feed streams enter into a block and get mixed, while blocks with external product stream are sinks. Note that splitting of source stream is not regarded as a splitting operation defined in this work because it could be achieved through the splitting fraction $z_{i,j,f}^{feedfrac}$ of source stream f into block $B_{i,j}$ and thus can be regarded as supplies of multiple source streams with the same specification.

The operation equipment (heaters/coolers, compressors/expanders) is embedded in the block superstructure through auxiliary units. To represent the pressurizing/depressurizing operation, both direct connecting streams and jump connecting streams are assigned with compressor or expander (only one of them would be selected). The inlet pressure for compressors/expanders is block pressure $P_{i,j}$ when direct/jump connecting streams are outlet flow from $B_{i,j}$. $P_{i,j}$ is also the outlet pressure for movers when direct/jump connecting streams are inlet flow to $B_{i,j}$. The inlet temperature for these compressors/expanders arranged at outlet streams ($F_{i,j,k,d}$ and $J_{i,j,i',j',k}$) of $B_{i,j}$ is the block temperature $T_{i,j}$, which is also the common temperature of outlet streams from $B_{i,j}$. The heating and cooling operations are achieved through the heat duty $Q_{i,j}^{h}$and cold duty $Q_{i,j}^{c}$, which are obtained from the energy balance around block $B_{i,j}$.

The general block superstructure for FGN synthesis problem developed in Figure 2 can be reduced to block superstructure with smaller size if the number of intermediate pools is known beforehand. As

Preprints (www.preprints.org) | NOT PEER-REVIEWED | Posted: 5 February 2018 doi:10.20944/preprints201802.0025.v1

Peer-reviewed version available at Processes 2018, 6, 23; doi:10.3390/pr6030023

an illustrative example, we first consider the case without intermediate pools. Knowing certain number of sources and sinks together with their specification and requirement, the classical superstructure is built by connecting each source and sink and shown in Figure 3a. Here all stream heaters/coolers and expanders/compressors are ignored for representation simplicity. As is shown in Figure 3b, we use a $1 \times N$ block superstructure to incorporate the classical superstructure. In this case, the column number is directly equal to number of sinks ($J = PS$). Since there are no intermediate pools, row number $I = 1$. Each block serves as sink block, from which product streams are withdrawn. Meanwhile, each block could also function as feed block, where multiple types of source streams are fed. Specifically, taking the first sink block $B_{1,1}$ as an example, there could be at most FS number of source streams entering this block. The activation of connectivity between sources and sinks could be reflected by the feed fraction $z^{feedfrac}_{i,j,f}$ of different sources f. If the feed fraction $z^{feedfrac}_{i,j,f}$ of source stream at the sink block $B_{i,j}$ is zero, then there is no connectivity between the source f and the sink p in block $B_{i,j}$; source-sink connectivity exists as long as the feed fraction of source stream $z^{feedfrac}_{i,j,f}$ is nonzero. Besides, the horizontal connecting streams between adjacent blocks in Figure 3b are also allowed. This additional feature physically indicates the material flowing between two fuel gas sinks.

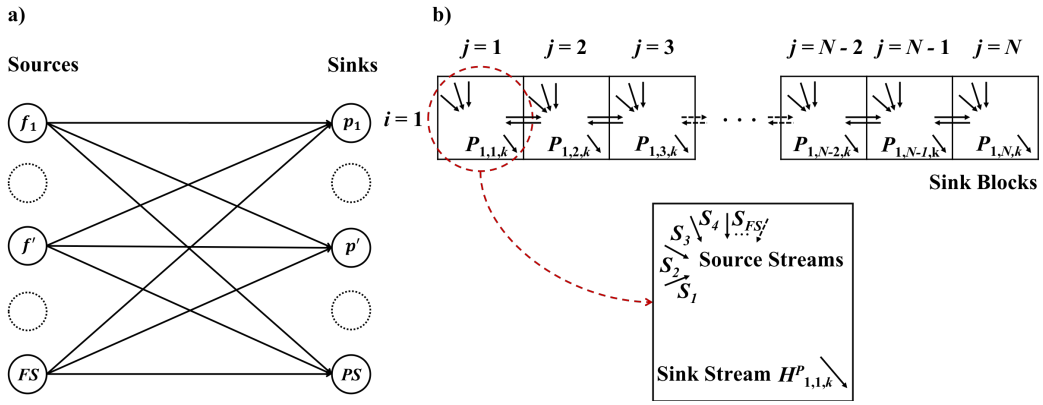

Figure 3. Block representation for fuel gas network problem: **(a)** Classical superstructure for fuel gas network. **(b)** Equivalent block superstructure for fuel gas network.

As for the more general case of fuel gas network superstructure, between the sources and sinks layer, there is normally another layer consisting of L number of intermediate pools, as is shown in Figure 4. Source streams first come into the intermediate pools, where certain operations such as mixing, purifying are executed according to different sink requirements. The outlet streams coming from the intermediate pools are further directed to the sinks or to the other different pools (shown as the blue line in Figure 4a). One way to incorporate the general superstructure is to utilize a block superstructure with larger size so that pools (involving mixing and splitting operations) can be included into the system. With this new feature of intermediate pools, the updated block superstructure is shown in Figure 4b. The first row consists of L number of pool blocks and the second row consists of PS number of sink blocks. In this case, the number of columns can be taken as $J = max\{L, PS\}$. The existence of intermediate pools make the row number as $I = 2$, one row to accommodate pools and another row for sinks. The distribution of source streams into each pool blocks is achieved through splitting operation of source streams. In the first row, the jump products are withdrawn from each block as outlet streams of intermediate pools. Specifically, taking the first column of block superstructure in Figure 4b as an example, the jump product $J^P_{1,1,k}$ (the summation of all the jump connecting streams to other blocks from block $B_{1,1}$) is withdrawn and directed to other blocks as jump feeds. These jump feeds (from $J_{1,2,2,1,k}$ to $J_{1,J,2,1,k}$) are mixed in the second row at sink blocks and then taken as the final product $H^p_{2,1,k}$ (the overall component flowrate for all product stream p). When the number of sources, sinks and pools in the system is not that large, the current commercial solver could handle the FGN

Preprints (www.preprints.org) | NOT PEER-REVIEWED | Posted: 5 February 2018 doi:10.20944/preprints201802.0025.v1

Peer-reviewed version available at Processes 2018, 6, 23; doi:10.3390/pr6030023

design problem without the solution challenge. However, when a large-scale problem is considered, the column number of two rows in this two-dimension block superstructure may not be necessarily the same since we can fix the streams in redundant blocks as zero. This fixing ensures that the number of blocks in the first row is only equal to the number of pools assigned in the system and the number of blocks in the second row is equal to the number of sinks.

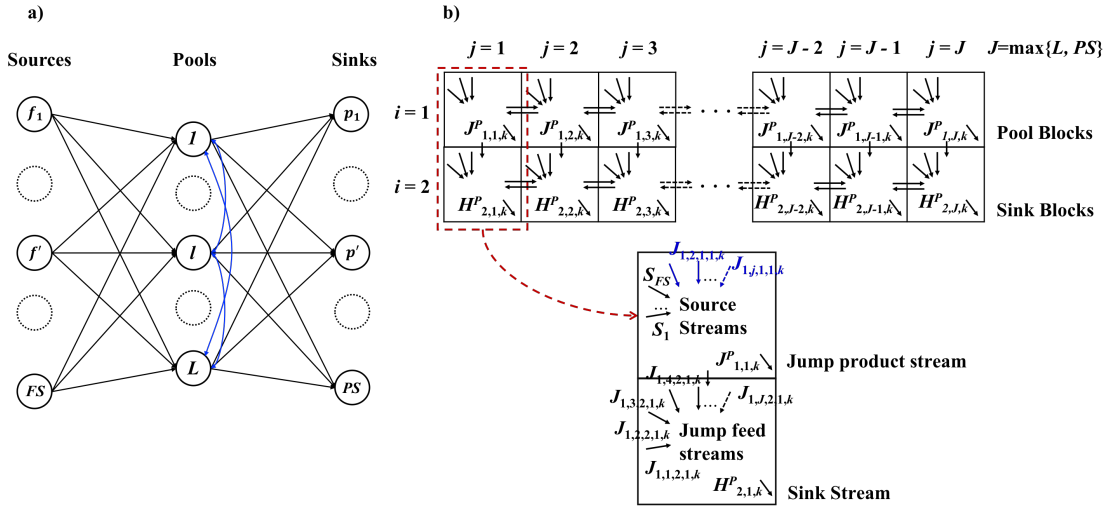

Figure 4. General superstructure for fuel gas network synthesis problem with intermediate pools: **(a)** General superstructure for fuel gas network with intermediate pools. **(b)** equivalent block superstructure.

As is discussed above, the block superstructure can be converted from the classical superstructure of fuel gas network. When there is no priori information provided on flow connectivity among sources, pools and sinks, the block superstructure can be constructed by simply setting the row number I and column number J (i.e., $J = max\{L,PS\}$), which then involves as many process alternatives as possible. The benefit for block representation method is on its generic feature that each block follows the same pattern with multiple inlet streams and outlet streams.

To this end, we introduced the block-based representation for fuel gas network synthesis problems. The illustrative example is on FGN synthesis with or without intermediate pools. We now develop the MINLP formulation for the FGN synthesis problem.

3. FGN Synthesis Problem Statement

This section gives the formal problem description for FGN synthesis problem using block superstructure. The sets given for this problem are the set $K = \{k|k = 1,...,|K|\}$ of components, the set $FS = \{f|f = 1,...,|FS|\}$ of fuel gas sources with component specification $y_{k,f}^{feed}$, a set $PS = \{p|p = 1,...,|PS|\}$ of fuel gas sinks with the material demand range as $\left[D_p^L, D_p^U\right]$, energy demand range as $\left[De_p^L, De_p^U\right]$, purity range as $\left[y_{k,p}^{min,prod}, y_{k,p}^{max,prod}\right]$ for species k as well as other quality specifications $\left[q_{s,p}^{min,prod}, q_{s,p}^{max,prod}\right]$ for quality s. The objective is to synthesize a fuel gas network that systemically utilizes the arrangement of fuel gas resources and minimizes the total annual cost. The set $D = \{d|d = 1,2\}$ designates the flow alignment. The flow alignment $d = 1$ when the stream is flowing in the horizontal direction, i.e., from block $B_{i,j}$ to $B_{i,j+1}$; $d = 2$ when the stream is flowing in the vertical direction, i..e., form block $B_{i,j}$ to $B_{i+1,j}$. The temperature range and flowrate range for all connecting flows including direct connecting flow and jump connecting flow is set as $\left[T^{min}, T^{max}\right]$ and $\left[FL, FU\right]$ respectively.

We consider the assumption for this work as constant properties (heat capacity, lower heating value, etc.), continuous steady-state operation, ideal gas condition, adiabatic expansion/compression, and ideal mixing. With this, we now provide the description of a MINLP model for fuel gas network synthesis based on block superstructure.

4. MINLP Model Formulation for Block-based Fuel Gas Network Synthesis

The main constraints for the MINLP model involve block material balance, flow directions, block energy balance, work calculation and task assignment/logic constraints. The objective of the FGN synthesis is to minimize the total annual cost.

4.1. Block Material Balance

The general material balance for each block $B_{i,j}$ considers the material flows of component k including horizontal inlet flow $F_{i,j-1,k,1}$, the horizontal outlet flow $F_{i,j,k,1}$, vertical inlet flow $F_{i-1,j,k,2}$, vertical outlet flow $F_{i,j,k,2}$, external feed stream $M^f_{i,j,k}$, external product stream $H^p_{i,j,k}$, jump feed flow $J^f_{i,j,k}$, and jump product flow $J^p_{i,j,k}$. Specifically, the material balance relation is presented as follows.

$$F_{i,j-1,k,1} - F_{i,j,k,1} + F_{i-1,j,k,2} - F_{i,j,k,2} + M^f_{i,j,k} - H^p_{i,j,k} + J^f_{i,j,k} - J^p_{i,j,k} = 0, \quad i \in I, j \in J, k \in K \tag{1}$$

The last four terms in the above relation are obtained though the following constraints.

$$M^f_{i,j,k} = \sum_{f \in FS} M_{i,j,k,f} \quad i \in I, j \in J, k \in K \tag{2}$$

$$H^p_{i,j,k} = \sum_{p \in PS} H_{i,j,k,p} \quad i \in I, j \in J, k \in K \tag{3}$$

$$J^f_{i,j,k} = \sum_{(i',j') \in LN} J_{i',j',i,j,k} \quad i \in I, j \in J, k \in K \tag{4}$$

$$J^p_{i,j,k} = \sum_{(i',j') \in LN} J_{i,j,i',j',k} \quad i \in I, j \in J, k \in K \tag{5}$$

All variables including $M^f_{i,j,k}$, $H^p_{i,j,k}$, $J^f_{i,j,k}$ and $J^p_{i,j,k}$ are obtained by summing multiple feeds or multiple products within single block $B_{i,j}$. The positive continuous variable $M_{i,j,k,f}$ indicates the amount of component flowrate k into block $B_{i,j}$ carried by feed stream f. The amount of component k taken from block $B_{i,j}$ through product stream p is designated by positive continuous variable $H_{i,j,k,p}$. The material flowrate for component k from block $B_{i,j}$ to $B_{i',j'}$ is $J_{i,j,i',j',k}$. The index i' and j' indicate row position and column position of a block $B_{i',j'}$ that is different from $B_{i,j}$. The subset $LN(i,j,i',j')$ designates the connection between block $B_{i,j}$ and block $B_{i',j'}$. It should be noted that for jump connecting flow $J_{i,j,i',j',k}$, $i \neq i'$ and $j \neq j'$ so as to avoid remixing in block $B_{i,j}$. The stream connectivities at the outer boundary of block superstructure are neglected by setting $F_{i=I,j,k,1} = F_{i,j=J,k,2} = 0$ to ensure that the interaction between the superstructure and the environment is only achieved through external feeds and products.

The flowrate $M_{i,j,k,f}$ for each feed f into block $B_{i,j}$ is completely or partially from the overall available amount F^{feed}_f. The distribution of feed stream f is achieved by the feed fraction $z^{feedfrac}_{i,j,f} \geq 0$ in block $B_{i,j}$. Hence $M_{i,j,k,f}$ can be determined as follows:

$$M_{i,j,k,f} = F^{feed}_f y^{feed}_{k,f} z^{feedfrac}_{i,j,f}, \quad i \in I, j \in J, k \in K, f \in FS \tag{6}$$

$$0 \leq \sum_{i \in I} \sum_{j \in J} z^{feedfrac}_{i,j,f} \leq 1, \quad f \in FS \tag{7}$$

Preprints (www.preprints.org) | NOT PEER-REVIEWED | Posted: 5 February 2018 doi:10.20944/preprints201802.0025.v1

Peer-reviewed version available at Processes 2018, 6, 23; doi:10.3390/pr6030023

Typically, headers receiving fuel gas have purity requirement for inlet streams to ensure correct operating conditions of corresponding equipment. This is achieved through the following inequality constraints:

$$y_{k,p}^{min,prod} \sum_{k' \in K} H_{i,j,k',p} \leq H_{i,j,k,p} \leq y_{k,p}^{max,prod} \sum_{k' \in K} H_{i,j,k',p}, \quad i \in I, j \in J, (k,p) \in kp \tag{8}$$

Here, the purity range for component k in product stream p is given by $[y_{k,p}^{min,prod}, y_{k,p}^{max,prod}]$. The set kp relates the key component k with product stream p with purity specifications. The product stream p have no purity restrictions when it does not appear in set kp.

On top of purity requirement of key component k in product stream p, possible requirement on ratio of different component k in product stream p is also considered.

$$P_{i,j,k=k',p} \geq \sum_{k'' \in K} \pi_{k',k'',p}^{prod} P_{i,j,k'',p} \quad i \in I, j \in J, p \in Ps \tag{9}$$

where $\pi_{k',k'',p}^{prod}$ is the minimum product ratio requirement between component k' and component k'' for product p.

We also impose the demand constraint for product p supplied to different headers:

$$D_p^L \leq \sum_{i \in I} \sum_{j \in J} \sum_{k \in K} H_{i,j,k,p} \leq D_p^U, \quad p \in PS \tag{10}$$

Here, D_p^L and D_p^U are minimum required amount and maximum allowed amount for product stream p respectively. Here depending on requirements of different fuel gas sinks, there are no information provided on D_p^L, D_p^U or both. In this case, we set $D_p^L = 0$ and $D_p^U = \max_{f \in FS} F_f^{feed}$.

Besides, energy demands De_p for each product stream p should be satisfied based on the following constraint:

$$\sum_{i \in I} \sum_{j \in J} \sum_{k \in K} H_{i,j,k,p} LHV_k \geq De_p, \quad p \in PS \tag{11}$$

where LHV_k refers to lower heating value for each component k, which measures energy content per unit mass or volume of pure combustible component.

Furthermore, each product stream should have acceptable limits on other certain specifications including lower heating value (LHV), reverse specific gravity ($1/SG$). Assuming that all the considered specifications are linearly additive based on mixture composition or have appropriate linear indices, the following constraint is supplied below for each product stream p [5].

$$q_{s,p}^{min,prod} \sum_{i \in I} \sum_{j \in J} \sum_{k \in K} H_{i,j,k,p} \leq \sum_{i \in I} \sum_{j \in J} \sum_{k \in K} H_{i,j,k,p} q_{s,k} \leq q_{s,p}^{max,prod} \sum_{i \in I} \sum_{j \in J} \sum_{k \in K} H_{i,j,k,p}, \quad p \in PS \tag{12}$$

Here the parameter $q_{s,k}$ denote the value of specification s for component k, and $[q_{s,p}^{min,prod}, q_{s,p}^{max,prod}]$ is the acceptable range of specification s for product stream p. Note that the quality specification $q_{s,k}$ is component flowrate-based instead of total flowrate-based, which is considered in the work of Hasan et.al. [5].

To obtain the total flowrate for all streams associated with the block $B_{i,j}$, we sum all components in each stream. Specifically, we obtain the toal flowrate $FP_{i,j,d}^T$, $FN_{i,j,d}^T$, $J_{i,j,i',j'}^T$, $M_{i,j,f}^T$, and $H_{i,j,s}^T$ from the component flowrate for $FP_{i,j,k,d}$, $FN_{i,j,k,d}$, $J_{i,j,i',j',k}$, $M_{i,j,k,f}$, and $H_{i,j,k,s}$ through the following relations.

$$FP_{i,j,d}^T = \sum_{k \in K} FP_{i,j,k,d}, \quad i \in I, j \in J, d \in D \tag{13}$$

$$FN^T_{i,j,d} = \sum_{k\in K} FN_{i,j,k,d}, \quad i \in I, j \in J, d \in D \tag{14}$$

$$J^T_{i,j,i',j'} = \sum_{k\in K} J_{i,j,i',j',k}, \quad (i,j,i',j') \in LN(i,j,i',j') \tag{15}$$

$$M^T_{i,j,f} = \sum_{k\in K} M_{i,j,k,f}, \quad i \in I, j \in J, f \in FS \tag{16}$$

$$H^T_{i,j,p} = \sum_{k\in K} H_{i,j,k,p}, \quad i \in I, j \in J, s \in PS \tag{17}$$

With the total flowrate information, we are able to model the splitting operation for achieving identical composition for all outlet streams including direction connecting streams, jump connecting streams and product streams. These relations are expressed through the following constraints:

$$FP_{i,j,k,d} = y^b_{i,j,k} FP^T_{i,j,d} \quad i \in I, j \in J, d \in D \tag{18}$$

$$FN_{i,j-1,k,1} = y^b_{i,j,k} FN^T_{i,j-1,1} \quad i \in I, j \in J \tag{19}$$

$$FN_{i-1,j,k,2} = y^b_{i,j,k} FN^T_{i-1,j,2} \quad i \in I, j \in J \tag{20}$$

$$J_{i,j,i',j',k} = y^b_{i,j,k} J^T_{i,j,i',j'} \quad (i,j,i',j') \in LN(i,j,i',j'), k \in K \tag{21}$$

$$H_{i,j,k,s} = y^b_{i,j,k} H^T_{i,j,s} \quad i \in I, j \in J, k \in K, s \in PS \tag{22}$$

Here the positive continuous variable $y^b_{i,j,k}$ refers to the block composition of component k. This block composition has the physical meaning as the composition of component k for all outlet streams from block $B_{i,j}$.

4.2. Flow Directions

The direct connectivity $F_{i,j,k,d}$ among adjacent blocks is a bidirectional flow with its positive component $FP_{i,j,k,d}$ and negative component $FN_{i,j,k,d}$. Only one of the component is active when the connecting flow $F_{i,j,k,d}$ is chosen to be nonzero. The selection of flow direction is a decision variable, which is achieved through the following binary variable:

$$z^{Plus}_{i,j,d} = \begin{cases} \text{True} & \text{if } F_{i,j,k,d} \text{ is from block } B_{i,j} \text{ to } B_{i,j+1} \ (d=1) \text{ or from block } B_{i,j} \text{ to } B_{i+1,j} \ (d=2) \\ \text{False} & \text{otherwise} \end{cases}$$

As a result, the flow direction determination is achieved though the following constraints:

$$F_{i,j,k,d} = FP_{i,j,k,d} - FN_{i,j,k,d} \quad i \in I, j \in J, k \in K, d \in D \tag{23}$$

$$FP_{i,j,k,d} \le FU z^{Plus}_{i,j,d}, \quad i \in I, j \in J, k \in K, d \in D \tag{24}$$

$$FN_{i,j,k,d} \le FU(1 - z^{Plus}_{i,j,d}), \quad i \in I, j \in J, k \in K, d \in D \tag{25}$$

4.3. Block Energy Balance

The involved enthalpy terms for block energy balance includes stream enthalpy, feed enthalpy, product enthalpy, external heating/cooling, work energy associated with expansion/compression. Then the steady-state energy balance for block $B_{i,j}$ is formulated as follows:

$$EF_{i,j-1,1} - EF_{i,j,1} + EF_{i-1,j,2} - EF_{i,j,2} + EM_{i,j} - EP_{i,j} + EJ^f_{i,j} - EJ^p_{i,j} + Q_{i,j} + W_{i,j} = 0, \ i \in I, j \in J \tag{26}$$

Preprints (www.preprints.org) | NOT PEER-REVIEWED | Posted: 5 February 2018 doi:10.20944/preprints201802.0025.v1

Peer-reviewed version available at Processes 2018, 6, 23; doi:10.3390/pr6030023

where, $EF_{i,j,d}$ represents the stream enthalpy carried by the material flow $F_{i,j,k,d}$ in flow direction d, $EM_{i,j}$ is the overall enthalpy brought into block $B_{i,j}$ along with feed streams , $EP_{i,j}$ is overall enthalpy taken away by product streams, $EJ^f_{i,j}$ is overall enthalpy carried into block $B_{i,j}$ through jump feed, $EJ^p_{i,j}$ is overall enthalpy taken out from block $B_{i,j}$ through jump product, $Q_{i,j}$ represents amount of heat/cold utility consumed in block $B_{i,j}$, $W_{i,j}$ indicates the amount of work energy added into or withdrawn from block $B_{i,j}$. These energy flow variables are shown in Figure 5.

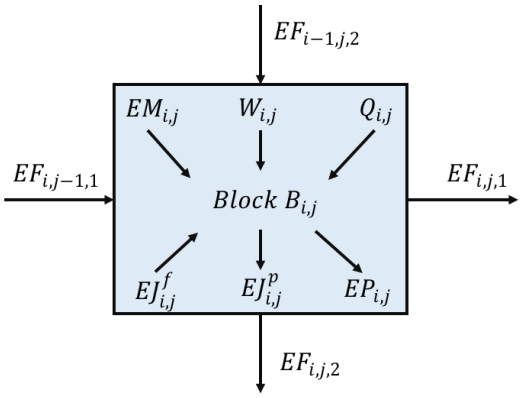

Figure 5. Illustration of energy balance on block $B_{i,j}$.

The stream enthalpy is determined as follows with the information provided on flowrate, component heat capacities and the block temperature. Depending on the flow direction, in flow alignment $d = 1$, the inlet temperature for block $B_{i,j}$ is either $T_{i,j}$ from block $B_{i,j}$ to $B_{i,j+1}$ or $T_{i,j+1}$ from block $B_{i,j+1}$ to $B_{i,j}$; in flow alignment $d = 2$, the inlet temperature for block $B_{i,j}$ is either $T_{i,j}$ from block $B_{i,j}$ to $B_{i+1,j}$ or $T_{i+1,j}$ from block $B_{i+1,j}$ to $B_{i,j}$.

$$EF_{i,j,1} = \sum_{k \in K} FP_{i,j,k,1} Cp_k T_{i,j} - \sum_{k \in K} FN_{i,j,k,1} Cp_k T_{i,j+1} \tag{27}$$

$$EF_{i,j,2} = \sum_{k \in K} FP_{i,j,k,2} Cp_k T_{i,j} - \sum_{k \in K} FN_{i,j,k,2} Cp_k T_{i+1,j} \tag{28}$$

where Cp_k is the heat capacity of component k.

The enthalpy amount brought into or withdrawn from block $B_{i,j}$ through jump flows are determined as follows:

$$EJ^f_{i,j} = \sum_{k \in K} \sum_{(i',j') \in LN} Cp_k T_{i',j'} J_{i',j',i,j,k} \qquad i \in I, j \in J \tag{29}$$

$$EJ^p_{i,j} = \sum_{k \in K} \sum_{(i',j') \in LN} Cp_k T_{i,j} J_{i,j,i',j',k} \qquad i \in I, j \in J \tag{30}$$

It should be noted that the inlet temperature of jump flow is always the temperature of source block $T_{i,j}$. Likewise, the feed enthalpy and product enthalpy are determined with the following constraints:

$$EM_{i,j} = \sum_{k \in K} \sum_{f \in F} M_{i,j,k,f} Cp_k T^f \qquad i \in I, j \in J \tag{31}$$

$$EP_{i,j} = \sum_{k \in K} \sum_{p \in P} P_{i,j,k,p} Cp_k T_{i,j} \qquad i \in I, j \in J \tag{32}$$

The amount of heat/cold utility consumed in block $B_{i,j}$ can be evaluated through the amount of heat introduced into ($Q^h_{i,j}$) or withdrawn from ($Q^c_{i,j}$) block $B_{i,j}$.

Preprints (www.preprints.org) | NOT PEER-REVIEWED | Posted: 5 February 2018 doi:10.20944/preprints201802.0025.v1

Peer-reviewed version available at Processes 2018, 6, 23; doi:10.3390/pr6030023

$$Q_{i,j} = Q^h_{i,j} - Q^c_{i,j} \tag{33}$$

The work energy can be also determined by the amount of work added into or taken out of block $B_{i,j}$, which are denoted as $W^{com}_{i,j}$ for compression and $W^{exp}_{i,j}$ for expansion respectively. The calculation of $W^{com}_{i,j}$ and $W^{exp}_{i,j}$ is explained later in this Section 4.6.

$$W_{i,j} = W^{com}_{i,j} - W^{exp}_{i,j} \tag{34}$$

Finally, to prevent condensation in the process integration network and ensure sufficient superheating, the following constraints are supplied for product stream p in block $B_{i,j}$ [5].

$$\sum_{k\in K} H_{i,j,k,p} Cp_k T_{i,j} \geq (MDP_p + \frac{5}{9}(5.15\frac{P_{i,j}}{100} - 312)\sum_{k\in K} H_{i,j,k,p} Cp_k \quad i \in I, j \in J, p \in PS \tag{35}$$

$$\sum_{k\in K} H_{i,j,k,p} Cp_k T_{i,j} \leq (HDP_p + \frac{5}{9}(2.33(\frac{P_{i,j}}{100})^2 - 2.8\frac{P_{i,j}}{100} - 305)\sum_{k\in K} H_{i,j,k,p} Cp_k \quad i \in I, j \in J, p \in PS \tag{36}$$

where parameter MDP_p is moisture dew-point temperature and parameter HDP_p is the hydrocarbon dew-point temperature for the product p.

4.4. Product Stream Assignments and Logical Constraints

We define binary variables for each product stream p at block $B_{i,j}$ to determine whether they are active in $B_{i,j}$ or not:

$$z^{product}_{i,j,p} = \begin{cases} 1 & \text{if product stream } p \text{ is withdrawn from block } B_{i,j} \\ 0 & \text{otherwise} \end{cases}$$

The identification of block as product block is achieved through the following logical relation, which involves product binary variable.

$$\sum_{k\in K} P_{i,j,k,p} \leq D^U_p z^{product}_{i,j,p} \quad i \in I, j \in J, p \in PS \tag{37}$$

For each block, there are at most one type of product stream present in block $B_{i,j}$. The logic proposition is illustrated as follows:

$$\sum_{p\in PS} z^{product}_{i,j,p} \leq 1 \quad i \in I, j \in J \tag{38}$$

Each product stream p appears in the block superstructure for at least once so as to ensure the supply of fuel gas header.

$$\sum_{i\in I}\sum_{j\in J} z^{product}_{i,j,p} \geq 1 \quad p \in PS \tag{39}$$

The temperature range for block with product stream p is from T^{min}_p to T^{max}_p.

$$T^{min}_p z^{product}_{i,j,p} + T^{min}(1 - z^{product}_{i,j,p}) \leq T_{i,j} \leq T^{max}_p z^{product}_{i,j,p} + T^{max}(1 - z^{product}_{i,j,p}) \quad i \in I, j \in J, p \in PS \tag{40}$$

Likewise, the pressure range for product block is $[P^{min}_p$ to $P^{max}_p]$.

Preprints (www.preprints.org) | NOT PEER-REVIEWED | Posted: 5 February 2018 doi:10.20944/preprints201802.0025.v1

Peer-reviewed version available at Processes 2018, 6, 23; doi:10.3390/pr6030023

$$P_p^{min} z_{i,j,p}^{product} + P^{min}(1 - z_{i,j,p}^{product}) \leq T_{i,j} \leq P_p^{max} z_{i,j,p}^{product} + P^{max}(1 - z_{i,j,p}^{product}) \quad i \in I, j \in J, p \in PS \quad (41)$$

4.5. Boundary Assignment

The boundary type between adjacent blocks can be either completely restricted or not. If there is no direct connecting stream between adjacent blocks, then the inter-block boundary is identified as completely restricted boundary. The decision of boundary type is achieved through the following binary variable $z_{i,j,d}^{cr}$.

$$z_{i,j,d}^{cr} = \begin{cases} 1 & \textit{If boundary between } B_{i,j} \textit{ and } B_{i,j+1} \textit{ for d=1 (between } B_{i,j} \textit{ and } B_{i+1,j} \textit{ for d=2)} \\ & \textit{is completetly restricted} \\ 0 & \textit{Otherwise} \end{cases}$$

According to the definition of completely restricted boundary, the following constraints are supplied to relate flowrate $F_{i,j,k,d}$ with boundary type.

$$F_{i,j,k,d} \leq FU(1 - z_{i,j,d}^{cr}), \quad i \in I, j \in J, d \in D \quad (42)$$

4.6. Work Calculation

The work term $W_{i,j}$ consists of compression work term $W_{i,j}^{com}$ and expansion work term $W_{i,j}^{exp}$. Both $W_{i,j}^{com}$ and $W_{i,j}^{exp}$ consist of work components for direct connecting streams ($W_{i,j,d}^{comp,FP}$ for positive component, $W_{i,j,d}^{comp,FN}$ for negative component), feed streams($W_{i,j,f}^{comp,FS}$), and jump connecting streams ($W_{i',j',i,j}^{comp,Jf}$). Accordingly,

$$W_{i,j}^{com} = \sum_{d \in D}(W_{i,j,d}^{comp,FP} + W_{i,j,d}^{comp,FN}) + \sum_{f \in FS} W_{i,j,f}^{comp,FS} + \sum_{(i',j') \in LN(i,j,i',j')} W_{i',j',i,j}^{comp,Jf}, \quad i \in I, j \in J \quad (43)$$

$$W_{i,j}^{exp} = \sum_{d \in D}(W_{i,j,d}^{exp,FP} + W_{i,j,d}^{exp,FN}) + \sum_{f \in FS} W_{i,j,f}^{exp,FS} + \sum_{(i',j') \in LN(i,j,i',j')} W_{i,j,i',j'}^{comp,Jp}, \quad i \in I, j \in J \quad (44)$$

We define the positive variable $PR_{i,j,d}^{F}$ to designate the pressure ratio between the block $B_{i,j+1}$ and $B_{i,j}$ for flow alignment $d = 1$ or between the block $B_{i+1,j}$ and $B_{i,j}$ for flow alignment $d = 2$. The calculation of $PR_{i,j,d}^{F}$ is activated when the boundary of block $B_{i,j}$ is not completely restricted at the corresponding flow alignment d ($z_{i,j,d}^{cr}$=0). Otherwise, the pressure ratio is taken as 1 to avoid the calculation of the pressure ratio. In horizontal direction, the pressure ratio is determined as follows:

$$\frac{P_{i,j+1}}{P_{i,j}} - PR^{up} z_{i,j,1}^{cr} \leq PR_{i,j,1}^{F} \leq \frac{P_{i,j+1}}{P_{i,j}} + PR^{up} z_{i,j,1}^{cr} \quad i \in I, j \in J \quad (45)$$

$$1 - PR^{up}(1 - z_{i,j,1}^{cr}) \leq PR_{i,j,1}^{F} \leq 1 + PR^{up}(1 - z_{i,j,1}^{cr}) \quad i \in I, j \in J \quad (46)$$

Here, PR^{up} is taken as the maximum pressure ratio, which is determined as P^{max}/P^{min}. Similarly, in vertical direction, the pressure ratio is determined as follows:

$$\frac{P_{i+1,j}}{P_{i,j}} - PR^{up} z_{i,j,2}^{cr} \leq PR_{i,j,2}^{F} \leq \frac{P_{i+1,j}}{P_{i,j}} + PR^{up} z_{i,j,2}^{cr} \quad i \in I, j \in J \quad (47)$$

$$1 - PR^{up}(1 - z_{i,j,2}^{cr}) \leq PR_{i,j,2}^{F} \leq 1 + PR^{up}(1 - z_{i,j,2}^{cr}) \quad i \in I, j \in J \quad (48)$$

Preprints (www.preprints.org) | NOT PEER-REVIEWED | Posted: 5 February 2018 doi:10.20944/preprints201802.0025.v1

Peer-reviewed version available at Processes 2018, 6, 23; doi:10.3390/pr6030023

For feed stream f, the pressure ratio is taken as the ratio between block pressure $P_{i,j}$ and parameter P_f^{feed} for feed pressure .

$$PR_{i,j,f}^{feed} = \frac{P_{i,j}}{P_f^{feed}} \quad i \in I, j \in J, f \in FS \tag{49}$$

From these pressure ratio definitions, we calculate the isentropic work on direct connecting streams, feed streams and jump connecting streams. In the horizontal direction, the inlet isentropic work is determined as follows:

$$\eta W_{i,j,1}^{comp,FP} - W_{i,j,1}^{exp,FP}/\eta = \sum_{k\in K} FP_{i,j-1,k,1} T_{i,j-1,1}^{s} R_{gas} \frac{\gamma}{\gamma-1}\{(PR_{i,j-1,1}^{F})^{\frac{\gamma-1}{\gamma}} - 1\} \quad i \in I, j \in J \tag{50}$$

$$\eta W_{i,j,1}^{comp,FN} - W_{i,j,1}^{exp,FN}/\eta = \sum_{k\in K} FN_{i,j,k,1} T_{i,j,1}^{s} R_{gas} \frac{\gamma}{\gamma-1}\{(\frac{1}{PR_{i,j,1}^{F}})^{\frac{\gamma-1}{\gamma}} - 1\} \quad i \in I, j \in J \tag{51}$$

Here R_{gas} is the gas constant and γ is the adiabatic compression coefficient. η is the adiabatic compression efficiency. Similarly, the isentropic work for a vertical entering stream is calculated as follows:

$$\eta W_{i,j,2}^{comp,FP} - W_{i,j,2}^{exp,FP}/\eta = \sum_{k\in K} FP_{i-1,j,k,2} T_{i-1,j,2}^{s} R_{gas} \frac{\gamma}{\gamma-1}\{(PR_{i-1,j,2}^{F})^{\frac{\gamma-1}{\gamma}} - 1\} \quad i \in I, j \in J \tag{52}$$

$$\eta W_{i,j,2}^{comp,FN} - W_{i,j,2}^{exp,FN}/\eta = \sum_{k\in K} FN_{i,j,k,2} T_{i,j,2}^{s} R_{gas} \frac{\gamma}{\gamma-1}\{(\frac{1}{PR_{i,j,2}^{F}})^{\frac{\gamma-1}{\gamma}} - 1\} \quad i \in I, j \in J \tag{53}$$

The work terms related to feed streams and jump connecting streams are calculated in a similar way:

$$\eta W_{i,j,f}^{comp,FS} - W_{i,j,f}^{exp,FS}/\eta = \sum_{k\in K} M_{i,j,k,f} T_f^{feed} R_{gas} \frac{1}{n_{fs}}\{(PR_{i,j,f}^{feed})^{n_{fs}} - 1\} \quad i \in I, j \in J, f \in FS \tag{54}$$

$$\eta W_{i,j,i',j'}^{comp,JF} - W_{i,j,i',j'}^{exp,JF}/\eta = J_{i,j,i',j'}^{T} T_{i,j} R_{gas} \frac{\gamma}{\gamma-1}\{(\frac{P_{i',j'}}{P_{i,j}})^{\frac{\gamma-1}{\gamma}} - 1\} \quad (i,j,i',j) \in LN(i,j,i',j') \tag{55}$$

Here n_{fs} is the adiabatic compression coefficient.

4.7. Objective Function

We consider the components of economic objective in the work of Hasan et al. [5] and derive the objective function for the FGN synthesis as follows.

$$\begin{aligned} \min \quad TAC = & \sum_{f\in FS}(\sum_{i\in I}\sum_{j\in J} UFC_f F_f^{feed} z_{i,j,f}^{feedfrac} + Di_f(F_f^{feed} - \sum_{i\in I}\sum_{j\in J} F_f^{feed} z_{i,j,f}^{feedfrac})) \\ & - \sum_{p\in PS} Rev_p(\sum_{k\in K} LHV_k \sum_{i\in I}\sum_{j\in J} H_{i,j,k,ps} - De_p) + \sum_{i\in I}\sum_{j\in J}\sum_{f\in FS} \pi_f F_f^{feed} z_{i,j,f}^{feedfrac} \\ & + CC^{HU}\sum_{i\in I}\sum_{j\in J} Qh_{i,j} + CC^{CU}\sum_{i\in I}\sum_{j\in J} Qc_{i,j} + CC^{exp}\sum_{i\in I}\sum_{j\in J} W_{i,j}^{exp} + CC^{com}\sum_{i\in I}\sum_{j\in J} W_{i,j}^{com} \end{aligned} \tag{56}$$

This objective function aims at minimizing total annual cost (TAC). Here parameter UFC_f is the unit cost of different source streams, Di_f is the unit cost of treatment cost for the remaining source stream, Rev_p is the unit profit from excess energy in product stream p. Besides, the parameter π_f denotes the unit transportation cost for source stream f. Parameters CC^{HU}, CC^{CU}, CC^{exp} and CC^{com} denote the

Preprints (www.preprints.org) | NOT PEER-REVIEWED | Posted: 5 February 2018 doi:10.20944/preprints201802.0025.v1

Peer-reviewed version available at Processes 2018, 6, 23; doi:10.3390/pr6030023

unit cost of heaters, coolers, expansion operations and compression operations, respectively. The first term in the objective function consists of source stream purchase cost and disposal cost. The second term corresponds to the profit gained from the released excess amount of energy in product stream p. The third term indicates the transporting cost of source streams. The last four terms refer to overall cost (both capital cost and operating cost) for heaters, coolers, expansion operations and compression operations.

5. Case Study

In this section, the fuel gas network synthesis problem with two scenarios are presented to demonstrate the application of block superstructure in synthesis of FGN. We consider two cases: case 1 for representation without intermediate pools; case 2 for representation with intermediate pools. The case study is from the work of Hasan et al. [5] and all problem instances are solved using ANTIGONE 1.1. [31] in GAMS 24.4 on a Dell Optiplex 9020 computer (Intel 8 Core i7-4770 CPU 3.4 GHz, 15.5 GB memory) running Springdale Linux.

5.1. Case Study Description

Although the definition of fuel gas network is taken from the literature (Hasan et al. [5]), the model we utilized in this work is not based on the total flowrate but the component flowrate. Because of the model discrepancy, we keep part of the source data from the literature in Table 1 and update required component parameters in Table 2. The sink data is directly taken from the literature without any changes and listed in Table 3. It should be noted that all the data have been converted to standard units.

Table 1. Sources streams specifications.

Specification/parameter	EFG	HPFG	TBOG	FFF
Adiabatic compression coefficient, n_{fs}	0.254	0.2	0.18	0.2
Availability, F_f^{feed} (kmol/s)	0.92938	0.05310	0.18255	<7.30229
Temperature, T_f^{feed} (K)	240	325	113	298
Pressure, P_f^{feed} (bar)	1.72369	7.58423	1.72369	26.20007
Methane, CH_4 (%)	60.0	81.0	92.0	85.0
Ethane, C_2H_6 (%)	0.0	6.0	0.0	5.0
Propane, C_3H_8 (%)	0.0	5.0	0.0	4.0
C_{3+} (%)	0.0	2.5	0.0	2.0
CO (%)	0.0	0.0	0.0	0.05
N2 (%)	40.0	5.5	8.0	3.95
Source unit cost, UFC_f ($/kmol)	0.0	0.0	0.0	4.184
Source disposal cost, Di_f ($/kmol)	0.209	0.292	0.209	0
Feed transporting cost, π_f ($/kmol)	0.0008	0.0008	0.0008	0.0008

Table 2. Component quality parameters.

Parameter	Methane	Ethane	Propane	C_{3+}	CO	N2
LHV(MJ/kmol)	800.234	1425.580	2041.113	2654.134	282.637	0
1/SG (28.96/mol wt)	1.8060	0.9636	0.6571	0.4985	1.0344	1.0342
Cp [KJ/(kmol K)]	37.16	57.40	80.30	114.93	29.20	29.15

Preprints (www.preprints.org) | NOT PEER-REVIEWED | Posted: 5 February 2018 doi:10.20944/preprints201802.0025.v1

Peer-reviewed version available at Processes 2018, 6, 23; doi:10.3390/pr6030023

Table 3. Specification for product streams (sinks).

Specification/parameter	C1	C2	C3	C4	C5
Energy demand, De_p (MJ/s)	152.309	149.378	120.305	149.378	87.921
Material demand, $[D_p^L, D_p^U]$ (kmol/s)	0.159 - 0.172	0.156 - 0.169	0.159 - 0.172	0.149 - 0.169	0.132 - 0.199
Temperature range, $[T_p^{min}, T_p^{max}]$ (K)	113-1000	113-1000	113-1000	113-1000	113-1000
Pressure range, $[P_p^{min}, P_p^{max}]$ (bar)	1.72-24.82	1.72-24.82	1.72-24.82	1.72-24.82	1.72-24.82
MDP_p (K)	277	277	277	277	277
HDP_p (K)	277	277	277	277	277
LHV(MJ/kmol)	264.885-8829.500	264.885-8829.500	264.885-8829.500	264.885-8829.500	264.885-8829.500
$1/SG$ (28.96/mol wt)	1.0-2.4	1.0-2.4	1.0-2.4	1.0-2.4	1.0-2.4
Methane, CH_4 (%)	>85.0	>85.0	>85.0	>85.0	>65.0
Ethane, C_2H_6 (%)	<15.0	<15.0	<15.0	<15.0	<15.0
Propane, C_3H_8 (%)	<15.0	<15.0	<15.0	<15.0	<15.0
C_{3+} (%)	<5.0	<5.0	<5.0	<5.0	<5.0
CO (%)	<10.0	<10.0	<10.0	<10.0	<10.0
N2 (%)	<15.0	<15.0	<15.0	<15.0	<15.0
Treatment factor, ψ_{sp}	1.0	1.0	1.0	1.0	1.0
Unit profit, Rev_p (\$/KJ)	0	0	0	0	6.6347×10^{-6}

There are totally four source streams (S_1, S_2, S_3, and S_4) and five sink streams (C_1, C_2, C_3, C_4, and C_5). S_1, S_2 and S_3 are gas streams from end flash gas (EFG), high-pressure fuel gas (HPFG), and tankage boil-off gas (TBOG) respectively. S_4 is supplied as the fuel from feed (FFF) because S_1, S_2, S_3 would not be enough to meet the complete energy demand of LNG plant. The five sinks are clarified according to similarity of specification among fourteen units [four gas turbine generators (GTG) for power generation, two gas turbine drivers (GTDs) for the propane cycle, three GTDs for the mixed refrigerant (MR) cycle, and five boilers] that consume fuel in the plant. Table 4 lists the cost parameter including capital expenditure (CAPEX) and operating expenditure (OPEX) for various FGN units (heaters/coolers, and compressors/expanders). Finally, we assign temperature lower bound as T^{min}=113 K, temperature upper bound as T^{max}=1000 K. The transporting cost for each source stream f is $\pi_f = 8.37 \times 10^{-4}$ \$/kmol. The operating time per year is 365 days.

Table 4. CAPEX and OPEX Coefficients for Various Equipment Units.

Unit	CAPEX (\$/KWh)	OPEX (\$/KWh)	Total (\$/KWh)
Compressor	10	0.01	CC^{com}=10.01
Expander	1	0.05	CC^{exp}=1.05
Heater	5	0.01	CC^{HU}=5.01
Cooler	5	0.02	CC^{CU}=5.02

5.2. Case 1: FGN Synthesis Without Pools

In this case, the block representation of FGN shown in Figure 3 is used. To avoid part of product stream recycled as feed into adjacent blocks through direct connecting flow, all the horizontal and vertical material flow, namely $F_{i,j,k,d=1}$ and $F_{i,j,k,d=2}$, are ignored for each product block. Accordingly, horizontal ($d = 1$) and vertical ($d = 2$) energy flow, $EF_{i,j,d}$, as well as their associated work terms are removed from energy balance. Also jump connecting streams from product blocks are fixed to be zero since they make the product blocks as intermediate pools.

The model for FGN without intermediate pools has 397 continuous variables, 49 binary variables, 845 bilinear terms, 243 signomial terms. The solution is obtained within 327 CPU seconds with optimal total annual cost as 70,136,064 \$/yr and optimality gap as 0.1%. The optimal solution reported in the literature [5] is 79,943,071 \$/yr. This 12.27 % reduction in TAC could be possibly attributed to the facts that: (1) we do not consider the nonlinear quality in this work, i.e., wobbe index, which brings less

Preprints (www.preprints.org) | NOT PEER-REVIEWED | Posted: 5 February 2018 doi:10.20944/preprints201802.0025.v1

Peer-reviewed version available at Processes 2018, 6, 23; doi:10.3390/pr6030023

strict requirement on network design; and (2) we consider expanders (ideal gas assumption) instead of valves (modeling based on real gas [5]) for expansion operation. The optimal block configuration for FGN and its corresponding optimal network are shown in Figure 6a and 6b respectively.

In the block representation of the optimal result (Figure 6a), the block $B_{1,1}$ takes compressed streams from source EFG, HPFG, and TBOG and expanded stream from source FFF while supplying sink stream to header C_4. Both the block $B_{1,2}$ and block $B_{1,3}$ collect part of compressed streams from source HBFG and TBOG and expanded stream from source FFF to generate sink stream for header C_1 and C_5 respectively. In block $B_{1,4}$, partial compressed streams from source EFG and TBOG mix with expanded stream from source FFF. This block yields the sink stream for header C_2. The block $B_{1,5}$ blend streams from source EFG and TBOG to yield a product stream for header C_3.

This obtained block representation is converted into FGN network shown in Figure 6b. It utilizes both HPFG and TBOG fully. Among all sink streams, only C_4 uses all source streams EFG, HPFG, TBOG, FFF while C_1, C_5 only use HPFG, TBPG, and FFF as source streams. Sink C_2 blends streams from EFG, HPFG, and TBOG. Sink C_3 takes source streams from EFG, and TBOG. It should be noted that both C_2 and C_3 accept part of EFG. The whole FGN network only could utilize 2.716% of EFG and the rest of it goes to flare. The reason is that EFG contains low methane (60%) and high inert content (40%). To utilize EFG as much as possible, it should be mixed with other source streams; however, such mixing could bring unacceptable large flows to sinks so EFG is only partially utilized in the system. Considering the price for FFF, none of sinks are taking it alone and sink C3 does not use FFF at all.

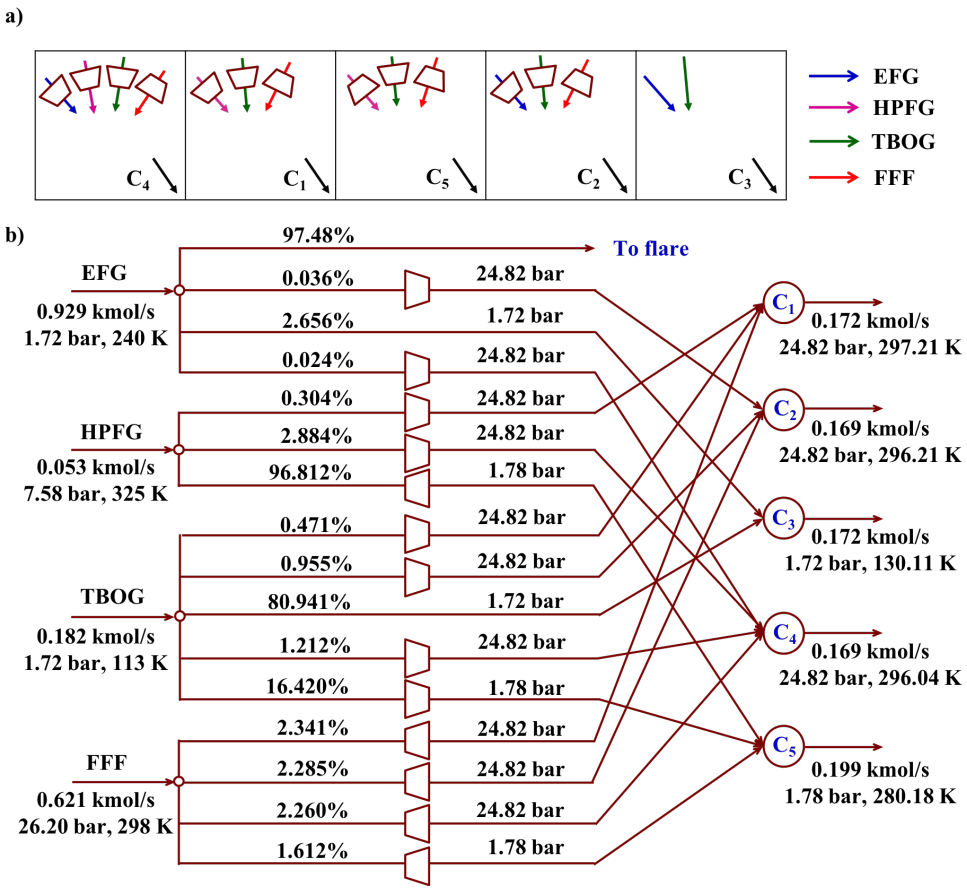

Figure 6. Block representation and process flowsheet for the optimal solution of FGN without intermediate pools: (**a**) Block representation for the optimal solution of FGN. (**b**) process flowsheet for the optimal solution of FGN.

The optimal header pressures are 24.82, 24.82, 1.72, 24.82, and 1.78 bar for header C_1-C_5. The flow rate of sink stream at headers at C_1-C_5 are 0.172, 0.169, 0.172, 0.169, 0.199 kmol/s respectively. The optimal header temperatures are reported as 297.21, 296.21, 130.11, 296.04, 280.18 K for header C_1-C_5 respectively. HPFG needs expanders before mixing with TBOG (1.72 bar) and FFF (1.72 bar) in C_5 because of its high pressure (7.58 bar). Similarly, all the FFF (26.20 bar) needs compressors so as to mix with other flows in C_1, C_2, C_4 and C_5. However, EFG and TBOG do not need any compressors or expanders before entering C_3, which are at 1.72 bar.

5.3. Case 2: FGN Synthesis With Pools

To investigate the influence of existence of pools on improving the economic performance of FGN, we use the representation shown in Figure 4. The material balance involving jump connecting streams is utilized to build connection between pool blocks and product blocks. For the jump product $J^p_{i,j,k}$ withdrawn from the pool block, it is distributed back into other pool blocks or product block. To avoid self-recycle of the jump product, the jump feed coming from the same block is fixed to be zero, $J_{i,j,i',j',k} = 0$, where $i = i'$ and $j = j'$. External feed streams are only allowed to enter into the first row with pool blocks while external product streams are only withdrawn from the second row with sink blocks.

We solve the model for FGN with intermediate pools using ANTIGONE as the MINLP solver. The model contains 1741 continuous variables, 71 binary variables, 9517 bilinear terms and 1621 signomial terms. The comparison of model statistics for these two cases are summarized in Table 5. The solution is obtained within 2136 CPU seconds with optimal total annual cost as 69,281,438 \$/yr and optimality gap as 0.1%. The involvement of intermediate pools results in a reduction of total annual profit by 1.22%, compared to the one reported as 70,136,064 \$/yr for the fuel gas network without intermediate pools. Figure 7 shows the optimal fuel gas network configuration.

Table 5. Summary of model statistics for case 1 and case 2.

	Case 1	Case 2
Continuous variable	397	1741
Binary variable	49	71
Bilinear terms	845	9517
Signomial terms	243	1621
CPU time (second)	327	2136
Solution (MM\$/yr)	70.1	69.3

The obtained block representation for the FGN is given in Figure 7a. Feed stream EFG is distributed into block $B_{1,3}$ and $B_{1,4}$. Part of feed stream HPFG is expanded and then enters into block $B_{1,4}$ while extra amount distributes into block $B_{1,2}$. In addition, feed stream TBOG is partially supplied to block $B_{1,3}$ and block $B_{1,5}$. Some other amount of TBOG is compressed and then enter block $B_{1,1}$. The feed stream FFF only enters the block $B_{1,1}$ after expanding operation. The blocks $B_{1,j}$ in the first row (column number j ranges from 1 to 5) collect the mixed stream and yield the jump product which are supplied as jump feed in the second row. Hence, these blocks are identified as intermediate pools, i.e., P_1, P_2, P_3, P_4, and P_5. At the second row of the block representation, the jump product from block $B_{1,1}$ and block $B_{2,4}$ mix at block $B_{2,1}$, which supplies product stream to sink C_1 and generates jump product entering block $B_{2,5}$. The block $B_{2,2}$ blends the jump product from block $B_{1,3}$ and $B_{1,5}$ to obtain sink stream C_3. The jump product from block $B_{1,3}$ compress firstly. This compressed stream splits into two parts: one part mixes with jump product from block $B_{1,1}$ at block $B_{2,3}$, where the sink stream C_4 is generated; another part mixes with jump product from block $B_{1,1}$ at block $B_{3,4}$, where the sink stream C_2 is obtained. Besides, a jump product flow is withdrawn from block $B_{2,4}$ and fed into block $B_{2,1}$. The jump product flows from block $B_{2,1}$, $B_{1,2}$ are compressed and mixed with other jump product flows from block $B_{1,4}$ and $B_{1,5}$ to supply the sink stream C_5.

Preprints (www.preprints.org) | NOT PEER-REVIEWED | Posted: 5 February 2018 doi:10.20944/preprints201802.0025.v1

Peer-reviewed version available at Processes 2018, 6, 23; doi:10.3390/pr6030023

The corresponding network structure is shown in Figure 7b. The optimal network consumes both HPFG and TBOG fully. Since all the blocks in the first row embed the inlet flow for mixing, five pools can be identified. Pool P_1 accepts source stream from TBOG and FFF, which only supply feed to P_1. P_2 takes part of stream from source HPFG. P_3 blends streams from EFG and TBOG. Part of external stream from EFG and HPFG enter pool P_4 while P_5 only takes stream from source TBOG. The outlet flow from pool P_1 is distributed into sink C_1, C_2 and C_4. The outlet flows from pool P_2 and P_4 are directly transported to sink C_5. Sink C_2, C_3 and C_4 accept inlet flow withdrawn from pool P_3. Part of the outlet flow from pool P_5 is recycled back to pool P_4 and another is transported into sink C_3. Part of product streams from C_2 and C_1 are recycled back to C_1 and C_5. The utilization of EFG in the whole FGN network is only 4.51% and the rest of it goes to flare.

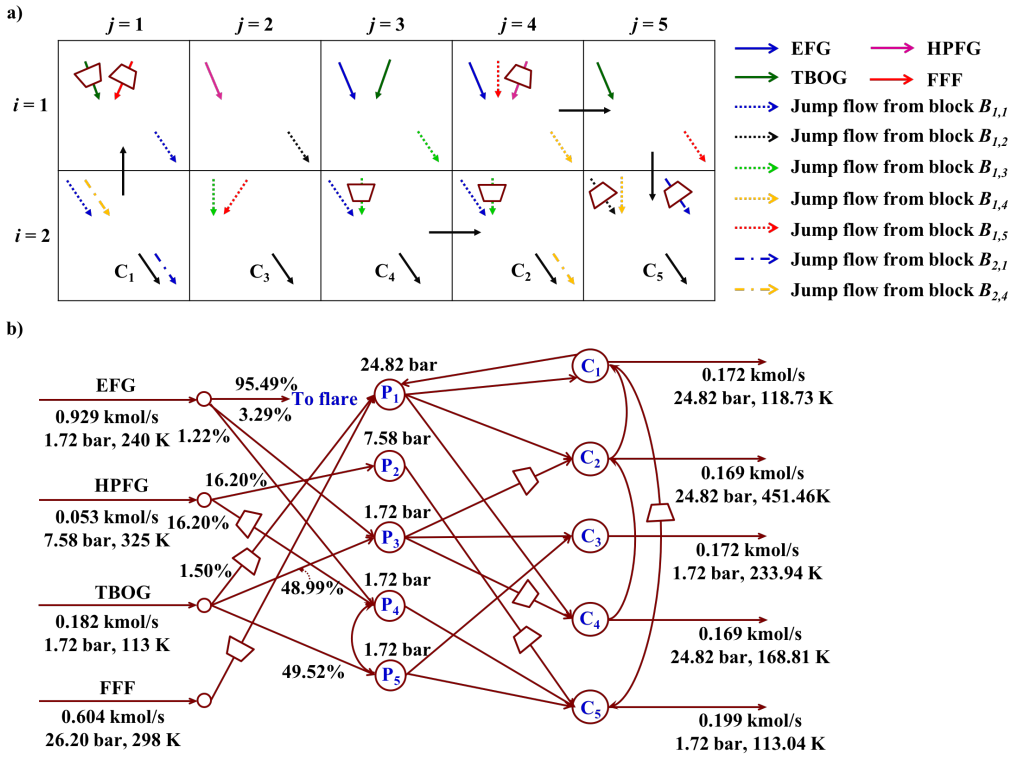

Figure 7. Block representation and process flowsheet for the optimal solution of FGN with intermediate pools: (**a**) Block representation for the optimal solution of FGN. (**b**) process flowsheet for the optimal solution of FGN.

The header pressures are 24.82, 24.82, 1.72, 24.82, and 1.72 bar for C_1-C_5 respectively. Expanders are arranged on inlet stream to P_4 from HPFG and inlet stream to P_1 from FFF. TBOG needs compressor before mixing with FFF in P_1 because of its low pressure (7.58 bar). Compressors are placed on the outlet streams of P_3 to sink C_2 and C_4 respectively. Expanders are arranged on the connecting stream from P_2 to sink C_5 as well as the stream from sink C_1 to sink C_5 so as to meet the pressure requirement. The temperature for sink stream C_1-C_5 are 118.73, 451.46, 233.94, 168.81 and 113.04 K. In addition, headers C_1-C_5 collect the flow rate of sink streams as 0.172, 0.169, 0.172, 0.169 and 0.199 kmol/s respectively.

To summarize for the case study section, the block-based representation method can effectively handle the fuel gas synthesis problem and the involvement of intermediate pools helps to improve the management of FGN network, which decreases the total annual cost.

6. Conclusions

We present an abstract superstructure representation for FGN synthesis, which is based on a block-based arrangement of source and sink. Each block allows multiple external fuel gas source streams and single fuel gas sink streams. The direct connecting streams between adjacent blocks and jump connecting streams among all blocks enable many alternative ways of flowing the mass and energy from sources to sinks. The blocks with multiple inlet streams serve as mixers and the blocks with multiple outlet streams are splitters. These blocks form a superstructure when arranged in a two-dimensional grid. The row number is determined by the number of intermediate pool layers and the number of sink layers. The column number is determined by the number of intermediate pools and the number of sinks. With the representation method, a MINLP model for fuel gas synthesis problem was proposed with constraints on material balance, energy balance, flow directions, and work calculation. A case study from LNG plant was presented for two instances: one without intermediate pools and another with intermediate pools. It was shown that the fuel gas network with pools could significantly reduce the total annual cost by 1.22%, compared to the fuel gas network without intermediate pools. These case study revealed that the block-based representation method would enable the synthesis of fuel gas network and helps to find novel network design. Note that the block-based representation method is initially proposed for systematic process intensification, and then applied to process synthesis. The application of block-based approach for FGN integration suggests a general framework towards process intensification, integration and synthesis.

Acknowledgments: The authors gratefully acknowledge financial support from the U.S. National Science Foundation (NSF CBET-1606027).

Author Contributions: J.L., S.E.D and M.M.F.H. conceived the model and prepared the manuscript.

Conflicts of Interest: The authors declare no conflict of interest.

References

1. Demirel, S.E.; Li, J.; Hasan, M.M.F. Systematic process intensification using building blocks. *Computers & Chemical Engineering* **2017**, *105*, 2–38.
2. Tahouni, N.; Gholami, M.; Panjeshahi, M.H. Integration of flare gas with fuel gas network in refineries. *Energy* **2016**, *111*, 82–91.
3. Zhang, J.; Zhu, X.; Towler, G. A simultaneous optimization strategy for overall integration in refinery planning. *Industrial & Engineering Chemistry Research* **2001**, *40*, 2640–2653.
4. Pellegrino, J.; Brueske, S.; Carole, T.; Andres, H. Energy and Environmental Profile of the US Petroleum Refining Industry. Technical report, EERE Publication and Product Library, 2007.
5. Hasan, M.M.F.; Karimi, I.A.; Avison, C.M. Preliminary synthesis of fuel gas networks to conserve energy and preserve the environment. *Industrial & Engineering Chemistry Research* **2011**, *50*, 7414–7427.
6. *U.S. Department of Energy (DOE): Refinery Capacity 2017*; Number Energy Information Administration, 2017.
7. De Carli, A.; Falzini, S.; Liberatore, R.; Tomei, D. Intelligent management and control of fuel gas network. IECON 02. IEEE, 2002, Vol. 4, pp. 2921–2926.
8. Zhou, L.; Liao, Z.; Wang, J.; Jiang, B.; Yang, Y.; Du, W. Energy configuration and operation optimization of refinery fuel gas networks. *Applied Energy* **2015**, *139*, 365–375.
9. Zhang, J.; Rong, G. An MILP model for multi-period optimization of fuel gas system scheduling in refinery and its marginal value analysis. *Chemical Engineering Research and Design* **2008**, *86*, 141–151.
10. Zhang, J.; Rong, G.; Hou, W.; Huang, C. Simulation based approach for optimal scheduling of fuel gas system in refinery. *Chemical Engineering Research and Design* **2010**, *88*, 87–99.
11. White, D.C.; others. Advanced automation technology reduces refinery energy costs. *Oil & Gas Journal* **2005**, *103*, 45–53.
12. Ismail, O.S.; Umukoro, G.E. Global impact of gas flaring. *Energy and Power Engineering* **2012**, *4*, 290.
13. Fawole, O.G.; Cai, X.M.; MacKenzie, A. Gas flaring and resultant air pollution: A review focusing on black carbon. *Environmental Pollution* **2016**, *216*, 182–197.

14. Quan, C.; Gao, N.; Wu, C. Utilization of NiO/porous ceramic monolithic catalyst for upgrading biomass fuel gas. *Journal of the Energy Institute* **2017**.
15. Mokheimer, E.M.; Dabwan, Y.N.; Habib, M.A. Optimal integration of solar energy with fossil fuel gas turbine cogeneration plants using three different CSP technologies in Saudi Arabia. *Applied Energy* **2017**, *185*, 1268–1280.
16. Friedler, F. Process integration, modelling and optimisation for energy saving and pollution reduction. *Applied Thermal Engineering* **2010**, *30*, 2270–2280.
17. El-Halwagi, M.M. Pollution prevention through process integration. *Clean Products and Processes* **1998**, *1*, 5–19.
18. Jagannath, A.; Hasan, M.M.F.; Al-Fadhli, F.M.; Karimi, I.A.; Allen, D.T. Minimize flaring through integration with fuel gas networks. *Industrial & Engineering Chemistry Research* **2012**, *51*, 12630–12641.
19. Tahouni, N.; Gholami, M.; Panjeshahi, M. Reducing energy consumption and GHG emission by integration of flare gas with fuel gas network in refinery. *International Journal of Chemical, Nuclear, Materials and Metallurgical Eng* **2014**, *8*, 900–904.
20. Kondili, E.; Pantelides, C.; Sargent, R. A general algorithm for short-term scheduling of batch operations—I. MILP formulation. *Computers & Chemical Engineering* **1993**, *17*, 211–227.
21. Yeomans, H.; Grossmann, I.E. A systematic modeling framework of superstructure optimization in process synthesis. *Computers & Chemical Engineering* **1999**, *23*, 709–731.
22. Friedler, F.; Tarjan, K.; Huang, Y.; Fan, L. Graph-theoretic approach to process synthesis: axioms and theorems. *Chemical Engineering Science* **1992**, *47*, 1973–1988.
23. Friedler, F.; Tarjan, K.; Huang, Y.; Fan, L. Graph-theoretic approach to process synthesis: polynomial algorithm for maximal structure generation. *Computers & Chemical Engineering* **1993**, *17*, 929–942.
24. Bagajewicz, M.J.; Manousiouthakis, V. Mass/heat-exchange network representation of distillation networks. *AIChE Journal* **1992**, *38*, 1769–1800.
25. Bagajewicz, M.J.; Pham, R.; Manousiouthakis, V. On the state space approach to mass/heat exchanger network design. *Chemical Engineering Science* **1998**, *53*, 2595–2621.
26. Wu, W.; Henao, C.A.; Maravelias, C.T. A superstructure representation, generation, and modeling framework for chemical process synthesis. *AIChE Journal* **2016**, *62*, 3199–3214.
27. Wu, W.; Yenkie, K.; Maravelias, C.T. A superstructure-based framework for bio-separation network synthesis. *Computers & Chemical Engineering* **2017**, *96*, 1–17.
28. Li, J.; Demirel, S.E.; Hasan, M.M.F. Simultaneous Process Synthesis and Process Intensification using Building Blocks. *Computer Aided Chemical Engineering* **2017**, *40*, 1171–1176.
29. Demirel, S.E.; Li, J.; Hasan, M.M.F. A General Framework for Process Synthesis, Integration and Intensification. *Proceedings of the 13th International Symposium on Process System Engineering* **2018**, *Under Review*.
30. Li, J.; Demirel, S.E.; Hasan, M.M.F. Process Synthesis using Block Superstructure with Automated Flowsheet Generation and Optimization. *AIChE Journal* **2018**, *Under Review*.
31. Misener, R.; Floudas, C.A. ANTIGONE: algorithms for continuous/integer global optimization of nonlinear equations. *Journal of Global Optimization* **2014**, *59*, 503–526.